


RESEARCH ARTICLE

Transcriptional profiling reveals gene expression changes associated with inflammation and cell proliferation following short-term inhalation exposure to copper oxide nanoparticles

Pedro M. Costa¹ | Ilse Gosens² | Andrew Williams³ | Lucian Farcas¹ | Daniele Pantano⁴ | David M. Brown⁴ | Vicki Stone⁴ | Flemming R. Cassee^{2,5} | Sabina Halappanavar³ | Bengt Fadeel¹ 

¹Division of Molecular Toxicology, Institute of Environmental Medicine, Karolinska Institutet, Stockholm, Sweden

²National Institute for Public Health and the Environment, Bilthoven, The Netherlands

³Environmental Health Science and Research Bureau, Health Canada, Ottawa, Canada

⁴School of Life Sciences, Heriot-Watt University, Edinburgh, UK

⁵Institute for Risk Assessment Studies, Utrecht University, Utrecht, The Netherlands

Correspondence

Bengt Fadeel, Division of Molecular Toxicology, Institute of Environmental Medicine, Karolinska Institutet, Stockholm, Sweden.

Email: bengt.fadeel@ki.se

Funding information

European Commission, Grant/Award Number: 604305

Abstract

Our recent studies revealed a dose-dependent proinflammatory response to copper oxide nanoparticles (CuO NPs) in rats following short-term inhalation exposure for five consecutive days. Here transcriptomics approaches were applied using the same model to assess global gene expression in lung tissues obtained 1 day post-exposure and after a recovery period of 22 days from rats exposed to clean air or 6 hour equivalent doses of 3.3 mg m⁻³ (low dose) and 13.2 mg m⁻³ (high dose). Microarray analyses yielded about 1000 differentially expressed genes in the high-dose group and 200 in low-dose compared to the clean air control group, and less than 20 after the recovery period. Pathway analysis indicated cell proliferation/survival and inflammation as the main processes triggered by exposure to CuO NPs. We did not find significant perturbations of pathways related to oxidative stress. Upregulation of epithelial cell transforming protein 2 (*Ect2*), a known oncogene, was noted and ECT2 protein was upregulated in the lungs of exposed animals. Proliferation of alveolar epithelial cells was demonstrated based on Ki67 expression. The gene encoding monocyte chemoattractant protein 1 (or CCL2) was also upregulated and this was confirmed by immunohistochemistry. However, no aberrant DNA methylation of inflammation-associated genes was observed. In conclusion, we have found that inhalation of CuO NPs in rats causes upregulation of the oncoprotein ECT2 and the chemokine CCL2 and other proinflammatory markers as well as proliferation in bronchoalveolar epithelium after a short-term inhalation exposure. Thus, pathways known to be associated with neoplastic processes and inflammation were affected in this model.

KEYWORDS

epithelial cell hyperplasia, inflammation, nanoparticles, oncogene, transcriptomics

1 | INTRODUCTION

Copper oxide (CuO) nanoparticles (NPs) are manufactured for a broad range of industrial applications due to their unique features regarding electricity and heat conductivity, biocidal properties and others. As such, they are commonly found in many commercial products, such as electronic equipment, paints and processed wood (for an overview, see Karlsson, Toprak, & Fadeel, 2015). As for many other nanomaterials, inhalation is a route of exposure of major concern in the occupational setting (Kuhlbusch, Asbach, Fissan, Gohler, & Stintz, 2011). In fact, there is a general concern regarding the effects of micro-

and nano-sized particulate matter in air, due to potential links with human respiratory diseases (Seaton, MacNee, Donaldson, & Godden, 1995). However, while several in vitro studies have provided evidence that CuO NPs are particularly potent in comparison to other metal oxides in terms of triggering cytotoxicity and genotoxicity (Di Bucchianico et al., 2013; Karlsson, Cronholm, Gustafsson, & Möller, 2008; Perreault et al., 2012), less is known about the potential health risks of CuO NPs following inhalation.

Effective prediction of health risks associated with exposure to xenobiotics requires an understanding of the mechanisms by which a given agent induces toxicity and/or elicits a defensive response.

However, assessing the risk from exposure to engineered nanomaterials is still a challenge, and a deeper knowledge of the underlying biological mechanisms of nanomaterials is required. High-throughput omics-based approaches to address mechanisms of toxicity are emerging as an integrated component of a new systems biology or “systems toxicology” approach to risk assessment of substances including nanomaterials (Costa & Fadeel, 2016; Sturla et al., 2014). One of the main advantages of omics-based approaches is the fact that omics data sets are amenable to advanced computational analysis enabling both quantification and statistical validation. Furthermore, using global omics approaches, such as transcriptomics, proteomics or metabolomics, or a combination of these approaches, novel insights into the underlying mechanisms of nanomaterials can be obtained in an unbiased manner, and subtle effects or effects not readily captured by traditional toxicity assays can be determined (see, for example, Feliu et al., 2015; Gioria et al., 2016; Lucafò et al., 2013). However, while omics tools have provided unprecedented opportunities to record global changes at the molecular level (Costa & Fadeel, 2016), the application of omics data in risk assessment of nanomaterials is still in its infancy (Labib et al., 2016; Nikota et al., 2016). Nonetheless, as pointed out by Wilson et al. (2013), transcriptomics data can support risk assessment by corroborating existing information on mode or mechanism of action; moreover, as chemical risk assessment moves away from a single mechanism of action approach toward a toxicity pathway-based paradigm, omics data could be used to understand the complexities of pathways affected by chemicals that will impact human health risk assessment. Transcriptomics approaches also have limitations insofar as gene expression profiling does not provide information on post-translational changes; to this end, other, complementary techniques are required (Costa & Fadeel, 2016). Furthermore, care should be taken not to equate the abundance of mRNA transcripts with activity of the corresponding proteins. Finally, more research is needed to promote regulatory acceptance of omics-based approaches. Interestingly, in a recent case study to evaluate the utility of toxicogenomics in the risk assessment of the carcinogen, benzo[a]pyrene, Moffat et al. (2015) concluded that global gene expression analysis might serve as a relatively fast and cost-effective tool for hazard identification and preliminary evaluation of potential carcinogens, and their carcinogenic potency. However, as discussed recently, a major challenge facing the “systems toxicology” approach is how to link observed network perturbations to phenotypes (Hartung et al., 2017).

In a recent, short-term inhalation study of CuO NPs in rats, organ burden and pulmonary toxicity were assessed (Gosens et al., 2016). The results revealed acute lung inflammation and cellular damage in rats following exposure to CuO NPs for 5 days, with most alterations resolved after a recovery period of 3 weeks. The study provided information that could be relevant for risk assessment, including the identification of sensitive endpoints for acute effects such as lung inflammation. However, the mechanism of action was not specifically addressed. In the present study, we aimed at investigating the mechanisms behind the pulmonary responses to inhaled CuO NPs, using tissue samples from the previous study (Gosens et al., 2016). Specifically, we focused on: (1) analyzing transcriptional changes in the lungs of rats following CuO NP exposure and recovery; (2)

unraveling the main molecular pathways underlying exposure to CuO NPs; and (3) integrating molecular pathways with phenotypical changes to validate the results. We also asked whether epigenetic mechanisms could explain changes in gene expression through a targeted analysis of DNA methylation of selected inflammation genes. The combination of transcriptomics approaches with conventional toxicity endpoints could aid in the delineation of toxicity pathways and support health risk assessment.

2 | MATERIALS AND METHODS

2.1 | Nanomaterials

The CuO nanomaterial was supplied as a nano-sized (15–20 nm according to information provided by the manufacturer) black powder from PlasmaChem GmbH (Berlin, Germany). For detailed characterization by transmission electron microscopy, to determine the primary particle size and X-ray-excited Auger electron spectroscopy, to assess the chemical state of the copper, refer to Gosens et al. (2016), and see Supporting information Table S1 for a summary. While most of the material (core and surface) was in the CuO form, the latter analysis revealed a non-negligible presence of copper hydroxides, resulting from exposure to air. The generation of the aerosol and characteristics of the pristine particles and of the aerosol are summarized in Supporting Information.

2.2 | Animals

The animal study was performed as described in Gosens et al. (2016) and tissue samples analyzed in the present study were derived from that study. Briefly, adult male (8-week-old) Wistar Unilever outbred rats (strain HsdCpb:WU) were obtained from Harlan Netherlands b.v. (Horst, The Netherlands). Rats (332 ± 22 g) were acclimatized for 2 weeks in Macrolon type IV cages (two to five individuals per cage) with food and water supplied ad libitum. Exposure and tissue collection were conducted at the National Institute for Public Health (RIVM) at Bilthoven, The Netherlands, under permit number 201300190. Experimental procedures complied with the European directive on the protection of animals for scientific purposes (Directive 2010/63/EU).

2.3 | Experimental design

The exposure was conducted using the $C \times T$ protocol (as described in OECD Test Guideline 403) considering a 6 hour exposure equivalent per day (the maximum recommended), where C is the concentration (set at 10 mg m^{-3}) of exposure and T is the duration (time) of exposure. There is a linear relationship between lung burden and the exposure expressed as $C \times T$, justifying the $C \times T$ concept and expression of the dose as 6 hour concentration equivalents (Supporting information Figure S1 and Table S2). For a more detailed description of the rationale for the dose selection, see Gosens et al. (2016). In brief, rats were exposed nose-only to a target concentration of 10 mg m^{-3} and the dose was subsequently expressed as 6 hour concentration equivalents of 0, 0.6, 2.4, 3.3, 6.3 and 13.2 mg m^{-3} CuO NPs. Controls

were exposed to clean air. Exposure was done during 5 consecutive days, with assessment in two groups, 1 day after the final exposure at day 6 (T_6) and after a recovery period of 22 days, with sampling taking place at day 28 (T_{28}). The animals collected at T_6 and T_{28} are henceforth referred to as “exposed” and “recovery” groups, respectively. By studying the effects shortly after termination of the exposure as well as after a recovery period of 3 weeks, information could be gathered on the reversibility of acute effects. At each sampling time, animals (five per experimental treatment and timepoint) were killed and lung samples were collected. For the present study, samples from animals exposed to the 6 hour equivalent doses of 3.3 and 13.2 mg NPs m^{-3} were analyzed as described below, and we refer to these as “low” dose (LD) and “high” dose (HD), respectively.

2.4 | Histochemical analysis

The lungs were infused via the trachea with neutral aqueous phosphate-buffered 4% solution of formaldehyde as a fixative under a constant pressure of 20 cm water for 1 hour. Sections (5 μm thick) were then obtained from lungs fixed in neutral-buffered formalin and embedded in paraffin. Following deparaffination and rehydration, the sections were treated with a tetrachrome histochemical procedure to highlight fibers (to detect potential fibrosis) and mucins that combine the Alcian Blue and van Gieson's elastic stains. Briefly, lung sections were stained with Alcian Blue (pH 2.5) for acidic polysaccharides for 30 minutes; Weigert's iron hematoxylin for 10 minutes (differentiated in ferric chloride), rinsed in 95% v/v ethanol to remove excess iodine and counterstained with van Gieson's Acid Picro-Fuchsin for 2 minutes (Martins, Alves de Matos, Costa, & Costa, 2015). After rinsing, dehydration and clearing with xylene, the slides were mounted in DPX resinous medium. Analysis was performed with a Nikon Eclipse TE2000 microscope (Nikon Instruments, Amsterdam, The Netherlands). Cu was localized in lung histological sections through the rubeanic acid (dithiooxamide) method. In brief, sections were deparaffinated and rehydrated as described above and incubated overnight at 37°C in dithiooxamide working solution (final concentration 0.005% in 10% m/v sodium acetate from a 0.1% stock solution in absolute ethanol), rinsed in water and counterstained with Nuclear Fast Red. All washing steps and material rinsing were performed with ultrapure grade water ($>16.2 \Omega cm$) to avoid Cu cross-contamination.

2.5 | Immunohistochemistry

Tissue sections were deparaffinated and brought to water, rinsed in phosphate-buffered saline (PBS) and permeabilized for 15 minutes in 0.1% Triton X-100 in PBS. After rinsing with PBS, the sections were blocked with Image-iT FX signal enhancer (Thermo Fisher Scientific, Waltham, MA) for 30 minutes and again washed. Sections were incubated overnight with primary antibodies at 4°C, washed in PBS and incubated with the AlexaFluor 488 fluorochrome-tagged goat antirabbit IgG polyclonal antibody (Thermo Scientific) for 2.5 hours in the dark at room temperature. The sections were then rinsed and mounted with DAPI-containing VectaShield (Vector Laboratories, Peterborough, UK) and analyzed immediately. Rabbit antirat ECT2 polyclonal antibody (sc-1005; Santa Cruz Biotechnology, Dallas, TX), rabbit

antirat CCL2 antibody (PA-34505; Invitrogen, Carlsbad, CA) and the rabbit antirat Ki-67 (PA5-16785; Invitrogen) were employed as primary antibodies, on the basis of the microarray results, with working concentrations of 2, 20 and 2 $\mu g ml^{-1}$, respectively. Ki-67 expression was used as a marker of cell proliferation (Schlüter et al., 1993). For each marker, sections from three to five individuals per condition were analyzed and representative images are shown.

2.6 | Microarray hybridization

Total RNA was extracted from individual rat lung samples using the AllPrep DNA/RNA Mini kit for animal tissue (Qiagen, Hilden, Germany), following the manufacturer's instructions. Total RNA was quantified using a NanoDrop 2000 spectrophotometer (Thermo Fisher Scientific), and RNA quality and integrity was assessed with an Agilent 2100 Bioanalyzer (Agilent Technologies, Santa Clara, CA). All samples showed RNA integrity numbers above 7, which is regarded as adequate for microarray analyses (Schroeder et al., 2006). Details of the microarray procedures can be found in Halappanavar et al. (2015). In brief, labeled cDNAs and cRNAs were synthesized using the Linear Amplification Kit (Agilent Technologies) from 200 ng of total RNA per individual rat lung sample or Universal Rat Reference RNA (Agilent Technologies). T7 RNA polymerase-transcribed cRNA from experimental samples were labeled with Cyanine-5 and UMRR was labeled with Cyanine-3. An equimolar amount of UMRR cRNA was mixed with each experimental cRNA and was hybridized to Agilent SurePrint G3 Rat 8 \times 60 K microarrays (Agilent). After washing, microarray slides were scanned in a G250B scanner (Agilent). Data was retrieved using the Feature Extraction 10.7.3 software (Agilent). Data analysis is described below.

2.7 | DNA methylation analysis

The level of methylation in inflammation-related genes was determined by real-time polymerase chain reaction (RT-PCR) using a PCR array designed for 22 rat genes, based on the principle of impaired transcription of methylated genomic DNA that has been cleaved by restriction enzymes at methylation sites. DNA extraction was performed as described above (Qiagen). The EpiTect Methyl II PCR Array was used, coupled with the EpiTect Methyl II DNA restriction kit (Qiagen), following manufacturer instructions. Analysis was run on a 7500 model quantitative (q)RT-PCR system (Applied Biosystems, Foster City, CA), using the RT² SYBR Green qPCR Mastermix (Qiagen). The results are expressed as the percentage of methylated nucleotides per gene sequence.

2.8 | Bioinformatics analysis

All statistics and computational analyses were performed using the software R 3.2 (Ihaka & Gentleman, 1996) and the significant threshold was set at $\alpha = 0.05$. Analysis of DNA methylation data was conducted through the *t*-test adapted for multiple comparisons by applying the Bonferroni correction for false discovery rate (FDR), Pearson's product-moment correlation *r* statistics and heatmaps (on log-transformed data). Microarray data were analyzed as described in Halappanavar et al. (2015). Briefly, from a randomized block design (Kerr & Churchill, 2007) data were normalized through locally weighted scatterplot smoothing regression modeling. The microarray analysis of

variance package for R (Wu, Kerr, Cui, & Churchill, 2003) was used to determine the statistical significance of the differentially expressed genes (DEGs). The *Fs* statistic with residual shuffling (Cui, Hwang, Qiu, Blades, & Churchill, 2005) was used to test between-treatment effects and to obtain *p*-estimates, which were corrected for FDR for multiple testing (Benjamini & Hochberg, 1995). Fold-change ratios were based on the least-square means. Any given microarray probe (gene) was considered to be expressed if the signal was above background in at least four of five samples in one or more experimental conditions and differential regulation was considered significant if the FDR-corrected *P* < 0.05 and the normalized fold change (NFR) > 2. Hierarchical clustering was achieved through the Ward–Pearson's method using the EMA package for R (Servant et al., 2010). Venn diagrams were obtained using Venny 2.0 (<http://bioinfogp.cnb.csic.es/tools/venny/index.html>). Data were deposited in the NCBI Gene Expression Omnibus Database under accession number GSE86390.

Gene ontology (GO) enrichment and KEGG (Kyoto Encyclopedia of Genes and Genomes) pathway analyses (Kanehisa et al., 2014) on DEGs were performed using the software DAVID (Huang, Sherman, & Lempicki, 2009a, 2009b). Fold-enrichment was considered significant if >1.5. The significance of the pathways was estimated through a modification of Fisher's exact test termed EASE (Expression Analysis Systematic Explorer) score (α < 0.05) available through DAVID (Hosack, Dennis, Sherman, Lane, & Lempicki, 2003). Comparative causal networks pathway analysis (Krämer, Green, Pollard, & Tugeneich, 2014) was performed on DEGs using the Ingenuity Pathway Analysis (IPA) software (content version 24718999) software (license from Ingenuity Systems, Redwood City, CA, USA). The outputs were filtered by *P*(α) < 0.05 and activation Z-score > 2 or < -2.

3 | RESULTS

3.1 | Microarray analysis following short-term inhalation exposure to CuO nanoparticles

In a recent study (Gosens et al., 2016), rats were exposed to CuO NPs for 5 days, with 1 and 22 day post-exposure evaluations of (sub)acute

toxicity. The CuO NPs elicited acute lung inflammation, which had mostly resolved after the 3 week recovery period. No lung fibrosis was detected. To evaluate further the inflammatory response, we determined the expression of a panel of proinflammatory markers in the lungs using established protocols (Brown, Kanase, Gaiser, Johnston, & Stone, 2014). Liver samples were also examined as previous work has shown that certain NPs could cross the air–lung barrier and translocate to distal organs including the liver (Rinaldo et al., 2015). We noted a dose-dependent increase in mRNA expression of proinflammatory markers in the lungs while no changes were detected in the livers of exposed animals (Supporting information Tables S3 and S4).

To probe the mechanisms underlying the pulmonary effects of CuO NPs, we proceeded to examine lung tissue samples derived from the previous study by Gosens et al. (2016) for global gene expression changes using cDNA microarrays. Of approximately 30 000 probes on the microarray slide, 1038 were found to be dysregulated significantly in at least one experimental condition, relative to the control, most of which corresponded to upregulation of gene expression (Figure 1). The largest number of DEGs was found at 1 day post-exposure in the lungs of rats exposed to a 6 hour equivalent dose of 13.2 mg m^{-3} (HD), whereas the lowest number was observed in rats exposed to a 6 hour equivalent dose of 3.3 mg m^{-3} (LD) and allowed to recover for 22 days (Figure 1). The highest (87) recorded for any single gene in the lungs of rats exposed to HD 1 day post-exposure was for the c-c motif chemokine ligand 2 (*Ccl2*) (NM_001105822), encoding for CCL2, also termed monocyte chemoattractant protein-1, MCP-1 (Table 1). Metallothioneins 1A and 2A (*Mt1a*, *Mt2a*), whose upregulation is an anticipated response to increased levels of intracellular metal ions (Tuomela et al., 2013), were both upregulated in HD rats (4.6- and 3.4-fold, respectively), but only *Mt1a* in LD animals (twofold).

3.2 | Gene ontology enrichment and pathway analysis of the transcriptomics data

GO analyses of the microarray data revealed that of 24 genes related to inflammation (GO:0002526), 23 were upregulated in the lungs of rats exposed to 13.2 mg m^{-3} NPs 1 day post-exposure (NFR ranging

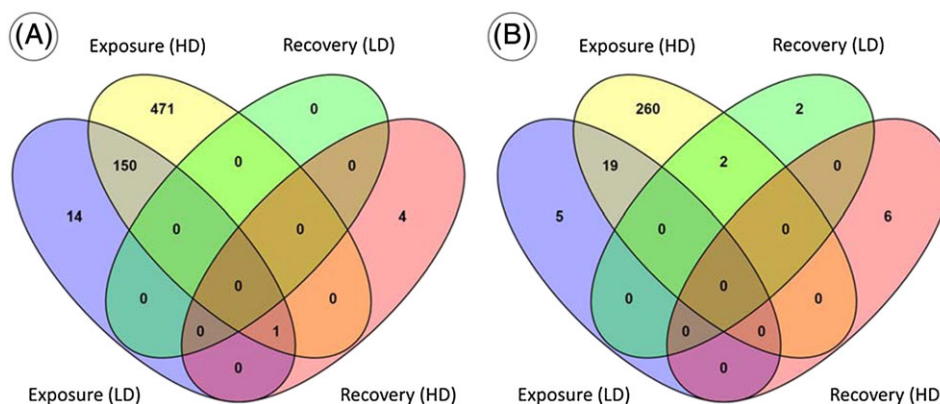


FIGURE 1 Microarray analysis of rat lung tissue following inhalation exposure to CuO nanoparticles. Venn diagrams of downregulated (A) or upregulated (B) genes that comply with at least twofold normalized change relatively to controls and FDR-corrected *P* < 0.05, for each experimental treatment, i.e. animals exposed to HD or LD CuO nanoparticles for 5 days and analyzed 1 day after the last exposure ("exposure") or after a recovery period of 22 days ("recovery"). HD, high dose; LD, low dose

TABLE 1 Summary of the most significantly up- and downregulated genes

	Accession	Gene	Gene name	FDR- <i>p</i>	NFC	Remarks
Exposure, 3.3 mg m ⁻³						
Upregulation	NM_130741	<i>Lcn2</i>	Lipocalin 2	≈0	19.3	Iron uptake and transport
Downregulation	NM_012666	<i>Tac1</i>	Tachykinin 1	≈0	-8.9	Intracellular signalling (cell adhesion-related)
Exposure, 13.2 mg m ⁻³						
Upregulation	NM_001105822	<i>Ccl2</i>	Chemokine (C-C motif) ligand 2/Monocyte chemoattractant protein 1	≈0	87.3	Pro-inflammatory response
Downregulation	NM_012666	<i>Tac1</i>	Tachykinin 1	≈0	-12.7	Intracellular signalling (cell adhesion-related)
Recovery (3.3 mg m ⁻³)						
Upregulation	NM_134418	<i>Gp2</i>	Glycoprotein 2 (zymogen granule membrane)	0.9194	3.0	Immune-related
Downregulation	NM_012543	<i>Dbp</i>	D site of albumin promoter (albumin D-box) binding protein	≈0	-4.3	Circadian rhythm regulation
Recovery (13.2 mg m ⁻³)						
Upregulation	NM_012543	<i>Dbp</i>	D site of albumin promoter (albumin D-box) binding protein	≈0	6.4	Circadian rhythm regulation
Downregulation	NM_012516	<i>C4bpa</i>	Complement component 4 binding protein, a	≈0	2.2	Immune-related

FDR-*p*, false discovery rate-corrected *P* value; NFC, normalized fold change relative to controls.

Rats were exposed via inhalation for 5 days to a low or high dose and analysis was done at day 1 post-exposure ("exposure") and after a recovery period of 22 days ("recovery").

between 2 and 11), with the exception of the *Klotho* gene (NM_031336.1), which was downregulated in animals subjected to this treatment. Interestingly, lipopolysaccharide-induced inflammation in rat lungs has previously been associated with downregulation of the *Klotho* gene (Ohshima et al., 1998). On the other hand, animals sampled at day 6, but subjected to the lowest dose, yielded only 10 deregulated genes from the same gene ontology, with consistently lower NFC values (2 and 4). Only one of the genes associated with the immune response was significantly dysregulated in animals exposed for 28 days and only at the highest dose, namely complement component 4 binding protein alpha (*C4bpa*) (NM_012516), NFC = 2. We then retrieved 25 pathways from the same gene list following KEGG analyses, of which 10 fitted the significance criteria (Table 2), altogether comprising approximately 100 genes (Figure 2). Overall, the mRNA levels of these genes yielded a similar pattern between animals exposed to either dose and collected at 1 day post-exposure, thus forming a cluster distinct to the animals collected following the recovery period (22 day post-exposure), which was mainly defined by upregulation of gene expression. The majority of the genes at 1 day post-exposure were related to immune response and cell cycle (Figure 2), in accordance with the results from the GO analysis, which showed that the most significant pathways were related to cell cycle and chemokine signaling pathways.

Pathway analysis performed using IPA yielded more detailed information on the molecular pathways, potentially activated by exposure to aerosolized CuO NPs. When comparing the disease and function pathways between the treatments, the most significantly activated (*Z*-score > 2) related to cell proliferation and inflammation, the exception being the pathway "concentration of lipids" in animals collected at 1 day post-exposure (Figure 3A). The results integrate pathways obtained from both in vivo and in vitro experiments with

pulmonary models or whole-lung tissue. The pathways related to "cell proliferation of carcinoma cell lines" were the most significantly activated of nine pathways (*Z* ≈ 3). None of the pathways was found activated in animals sampled after recovery (i.e., 22 day post-exposure). These observations prompted a search for genes associated with epithelial lung cell/cancer cell proliferation, the most significant of which was epithelial cell transforming protein (*Ect2*, BC168962), which was consistently present in the aforementioned pathways. The expression of this oncogene attained NFC 3.34 and 7.46 relative to control, in LD and HD rats at 1 day post-exposure, respectively, having returned to control levels following recovery, 22 days post-exposure. *Ccl2* was also consistently present in pathways related to inflammation such as cell migration, as well as cell proliferation pathways (Figure 3B), hence yielding a significant overlap with *Ect2*.

Using the IPA tool, the genes most significantly related to the upstream regulation of the identified pathways were *Nos2* and *Insig1*. The former reached a positive *Z*-score of 3.6 (activation) in HD animals at 1 day post-exposure (not significant in any other treatment), whereas the latter attained a *Z*-score of -3.8 (deactivation) in animals subjected to either dose (Figure 3A).

3.3 | Histopathological analysis and immunostaining for ECT2, Ki67 and CCL2

Next, histopathological evaluation and immunohistochemistry was performed to validate the microarray results. To this end, tissue samples from the previous study by Gosens et al. (2016) were analyzed. We noted an intrusion of immune cells into alveoli (indicating lung alveolitis) at 1 day post-exposure in a seemingly dose-response manner, returning to levels similar to control animals after recovery (Supporting information Figure S2), in line with our previous study

TABLE 2 KEGG pathway analyses of significantly deregulated genes

KEGG pathway term	No. genes	% coverage	Fold enrichment	Benjamini-corrected P value
rno04110:Cell cycle	17	2.27	2.969	0.022*
rno04062:Chemokine signalling pathway	20	2.67	2.574	0.016*
rno00900:Terpenoid backbone biosynthesis	6	0.80	9.432	0.012*
rno04610:Complement and coagulation cascades	12	1.60	3.773	0.009*
rno04940:Type I diabetes mellitus	10	1.34	3.668	0.037*
rno04621:NOD-like receptor signalling pathway	10	1.34	3.550	0.039*
rno05332:Graft-versus-host disease	9	1.20	3.884	0.036*
rno04612:Antigen processing and presentation	12	1.60	3.001	0.033*
rno04142:Lysosome	14	1.87	2.633	0.035*
rno04060:Cytosignificant kine-cytokine receptor interaction	19	2.54	2.123	0.045*
rno04623:Cytosolic DNA-sensing pathway	8	1.07	3.827	0.052
rno04514:Cell adhesion molecules (CAMs)	15	2.00	2.231	0.076
rno04620:Toll-like receptor signalling pathway	11	1.47	2.690	0.074
rno05330:Allograft rejection	8	1.07	3.322	0.089
rno00982:Drug metabolism	9	1.20	2.751	0.135
rno00760:Nicotinate and nicotinamide metabolism	5	0.67	4.784	0.150
rno04710:Circadian rhythm	4	0.53	6.772	0.144
rno05322:Systemic lupus erythematosus	10	1.34	2.445	0.144
rno00100:Steroid biosynthesis	4	0.53	5.178	0.254
rno03320:PPAR signalling pathway	8	1.07	2.480	0.251
rno05416:Viral myocarditis	9	1.20	2.277	0.250
rno05320:Autoimmune thyroid disease	7	0.93	2.525	0.309
rno00072:Synthesis and degradation of ketone bodies	3	0.40	7.336	0.312
rno00650:Butanoate metabolism	5	0.67	3.335	0.303
rno04914:Progesterone-mediated oocyte maturation	8	1.07	2.024	0.438

*Significant pathways (EASE $P < 0.05$ and fold enrichment > 1.5).

(Gosens et al., 2016). The inflammatory response tended to be focal in the lungs of animals exposed to either dose, although the foci were more disseminated and larger in animals exposed to the highest dose (13.2 mg m^{-3}). Overall, the two most significant alterations found in alveolar epithelia were intrusion of inflammatory cells (monocytes and macrophages) and proliferation of epithelial cells (the constituents of alveolar septa), in either case exhibiting the same dose-response pattern after the 5 days of exposure (Supporting information Figure S2A,C,E), subsequently returning to the normal condition, similar to the control animals (Supporting information Figure S2B,D,E). Additionally, epithelial cell hyperplasia was accompanied by hypertrophy of cells, thus contributing to the thickening of septa. Cell death was limited to necrotic macrophages in the most severe inflammatory foci in HD rats, but was never diffuse. Emphysema and fibrosis were rare or absent in the lungs of rats from either treatment (data not shown). The latter findings are fully in line with the previous report showing that emphysema was rare and fibrosis was absent (Gosens et al., 2016). Copper deposits were occasionally found in HD rats at 1 day post-exposure, being rare in LD animals and absent in the lungs of control animals or in the recovery group. These deposits were occasionally found in alveoli (extracellular deposits) or, more frequently, in immune cells (Supporting information Figure S2E).

We then determined the expression of Ki67 in the lung to corroborate increased cell proliferation, as well as the detection of the ECT2 and CCL2, which were both predicted to be upregulated based on the

microarray data. The ECT2 protein was successfully localized in alveolar epithelia (Figure 4) being present in the nuclei of cells of samples from all experimental treatments, including controls. This pattern of expression was expected, as ECT2 is known to regulate DNA synthesis and cytokinesis (Tatsumoto, Xie, Blumenthal, Okamoto, & Miki, 1999), processes that occur normally in type II alveolar cells. Interestingly, ECT2 was found to be increased in foci of hyperplastic cells, low-to-moderate in the case of LD-exposed animals at day 1 post-exposure, and strong expression was noted in the case of rats exposed to the HD at the same timepoint (Figure 4C,E). In contrast, the expression of ECT2 after the recovery period displayed a similar pattern to that of controls (Figure 4B,D,F). In the HD animals at day 1 post-exposure, the ECT2 protein was also localized in the cytoplasm, yielding a strong fluorescent signal, whereas this was less prominent in the LD animals. The same pattern was noted for Ki67, a marker of cell proliferation (Figure 5). When compared to controls (Figure 5A), LD and HD rats yielded a strong signal for the Ki67 protein in hyperplastic foci, particularly HD (Figure 5C,E), thereby confirming proliferation of alveolar epithelial cells, whereas after recovery, the epithelial expression returned to control values (Figure 5B,D,F). Similarly, CCL2 (Figure 6) was overexpressed in the lungs of LD and HD rats and yielded a strong signal in both epithelial and immune cells, mostly in hyperplastic foci (Figure 6 C,E), where CCL2 localized mostly within immune cells in controls (Figure 6A). CCL2 expression was higher in HD than in LD day 1 post-exposure, suggesting a dose-response, and normalized

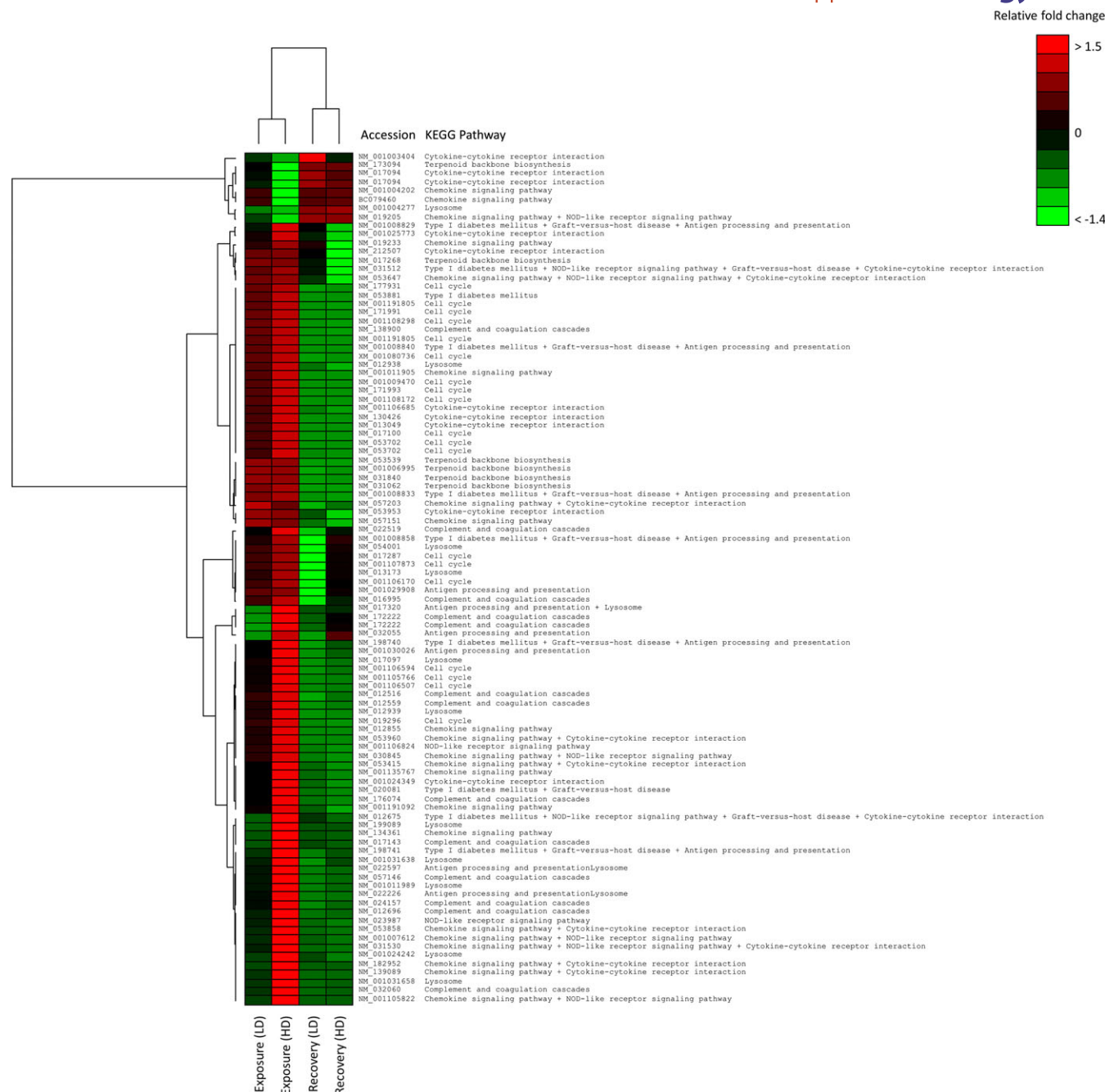


FIGURE 2 Heatmap illustrating the findings from the KEGG pathway analysis, which retrieved 98 genes pertaining to the pathways listed in Table 2. Cluster analysis was done through Ward's method employing Pearson's r as metric. Color scale was trimmed at $|1.5|$ to enhance contrast

after recovery (i.e., at day 22 post-exposure) (Figure 6B,D,F). Thus, the expression of *CCL2* and *ECT2* in lungs of rats exposed to CuO NPs was in agreement with the levels of transcripts of the respective genes (see Table 1).

3.4 | No evidence for epigenetic regulation of inflammation genes

Next, a targeted epigenetics study was conducted to address the potential role of DNA methylation in the regulation of inflammatory responses following exposure of rat lungs to CuO NPs. To this end, DNA methylation of a selected panel of inflammation-related genes was investigated using a PCR array. However, the levels of gene

methylation were overall low (typically totalling $<1\%$) and highly variable for all the genes that were investigated (Figure S3A). Among the 22 genes, only the Fas-associated death domain (*Fadd*) yielded a significant difference versus the controls (Supporting information Figure S3A), in LD animals evaluated at 1 day post-exposure, suggesting increased methylation (Supporting information Figure S3B). Nonetheless, no correlation was found between *Fadd* gene methylation and gene expression, as determined by our microarray analysis. When combining the methylation levels of all the analyzed genes, no significant differences were found between treatments, in spite of a trend towards reduced DNA methylation in animals exposed to HD at 1 day post-exposure. Overall, only marginal effects of DNA methylation on inflammation could be inferred and no significant correlations were found between

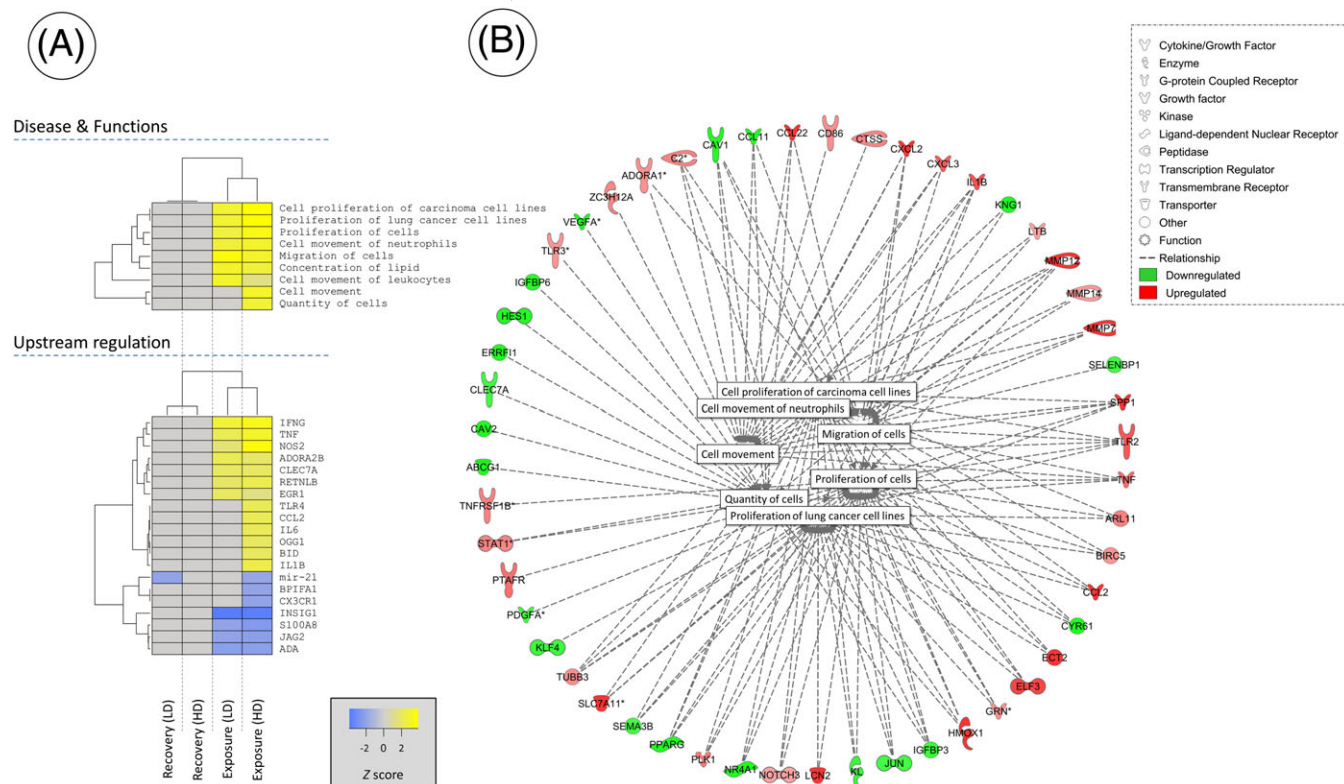


FIGURE 3 Ingenuity Pathway Analysis results. (A) Comparative analysis of disease and function pathways between the four experimental conditions, i.e., exposure for 5 days to a 6 hour equivalent dose of 13.2 (HD) and 3.3 (LD) mg m^{-3} CuO nanoparticles, respectively, plus recovery for 22 days after exposure to HD and LD for 5 days, and significant molecules integrating potential upstream regulation. (B) Transcriptional network of disease and function pathways retrieved from rats exposed to HD for 5 days. Significance thresholds were set at $|Z| > 2$ and $P < 0.05$. HD, high dose; LD, low dose

gene expression results retrieved from microarray experiments and the percentage of gene methylation (Pearson r , $P > 0.05$).

4 | DISCUSSION

We have found that short-term inhalation exposure of rats to CuO NPs results in acute lung inflammation (Gosens et al., 2016), and we also noted that this leads to the upregulation of proinflammatory cytokines in the lungs, while no such changes were detected in the liver of exposed animals. In the present transcriptomics study, we focused on the lungs, the primary target organ. Global gene expression analyses were thus performed on the lungs of rats exposed via inhalation for 5 consecutive days to two doses (LD and HD) of CuO NPs. Pathway analysis of the transcriptomics data showed that cell proliferation/survival and inflammation in rat lungs were the main processes affected by inhalation exposure to CuO NPs. Validation studies confirmed the upregulation of specific molecules, i.e., the oncoprotein, ECT2, and the chemokine, CCL2, in the lungs, while epithelial cell hyperplasia and cell proliferation was evidenced by conventional histological analysis and expression of the proliferation marker, Ki67. We also noted here and in our previous study (Gosens et al., 2016) that markers of emphysema and lung fibrosis were essentially absent in rats exposed to CuO NPs. Instead, our results suggest that the adverse outcomes of inhalation exposure of CuO NPs may be linked to the induction of inflammation and a concomitant proliferation of lung alveolar epithelial cells. Importantly, while lung

inflammation is in line with our previously published findings on short-term inhalation exposure to CuO NPs (Gosens et al., 2016), microarray analysis identified additional molecular responses that may serve to explain the mode of action of these NPs. In particular, the finding of epithelial cell proliferation is relevant as alveolar type II cells are known to be able to initiate lung adenocarcinoma, a major form of non-small cell lung cancer (Lin et al., 2012). However, one should not infer from these observations that a short-term inhalation exposure to CuO NPs would translate into lung cancer in rats or humans, as both the lung pathology and gene expression changes returned to normal after the recovery period. Nevertheless, the present findings suggest that studies of the potential impact of long-term exposure to CuO NPs on neoplastic processes are warranted.

Oxidative stress has previously been implicated as a major cause of CuO NP-induced cell death in both in vitro and in vivo models (Fahmy & Cormier, 2009; Jing, Park, Peters, & Thorne, 2015). However, our KEGG and IPA analyses of the microarray data did not yield evidence for pathways related to oxidative stress and genes related to oxidative stress were not among the most significantly dysregulated genes, nor did we detect significant changes in genes or pathways related to the promotion (or inhibition) of cell death. The latter results are supported by the paucity of apoptotic cells in alveolar epithelia of exposed animals. It should be noted that several markers of cell damage were detected in the bronchoalveolar lavage fluid obtained from rats at 1 day post-exposure in our previous study, including elevated levels of lactate dehydrogenase and total cellular protein, both markers of general cell damage, as well as elevated

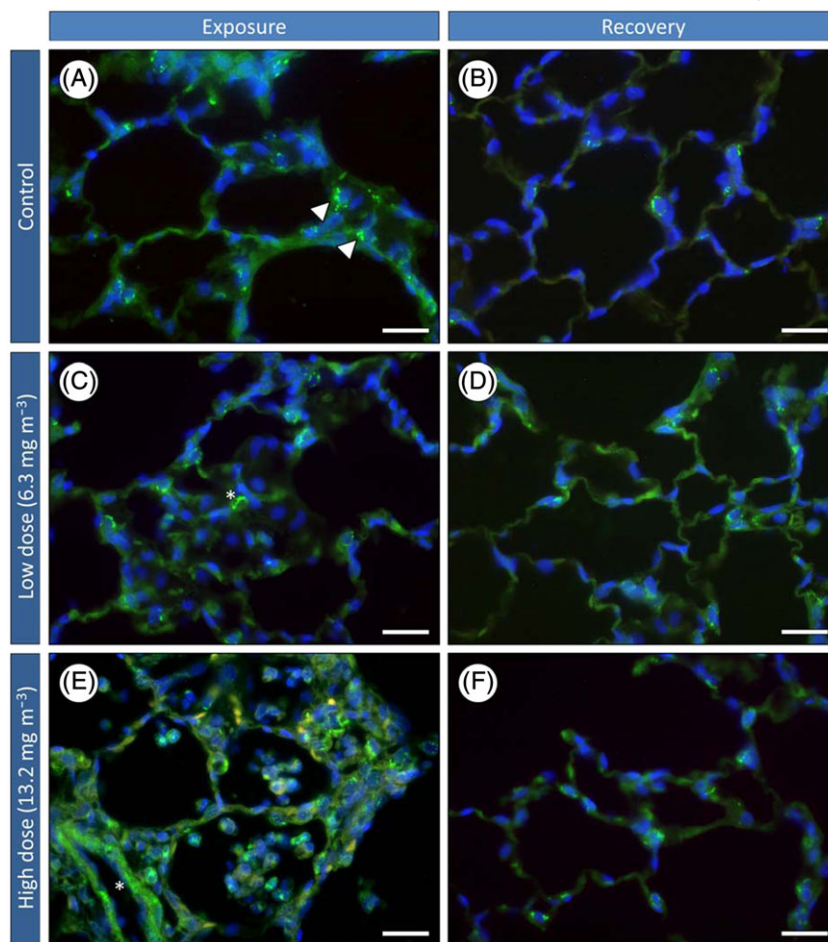


FIGURE 4 Expression of the oncoprotein, ECT2 in lung alveoli of control animals or rats exposed to CuO nanoparticles for 5 days at the indicated doses and analyzed 1 day post-exposure and after a recovery period of 22 days (day 28). Lungs of rats exposed to clean air as a control (A,B) and after a low-dose exposure (C,D) or after a high-dose exposure (E,F). Note the expression of ECT2 in the cytoplasm of epithelial cells (*), particularly in the lungs of high-dose animals. Scale bars: 25 μ m

gamma-glutamyl transferase levels, a marker for alveolar type II epithelial cell and/or bronchiolar secretory cell damage (Gosens et al., 2016). The changes in cell damage markers returned to baseline levels after the recovery period. However, cellular damage is not necessarily reflected at the transcriptional level and the present results in combination with our previous study underline the value of applying more than one method or endpoint when evaluating biological responses to NPs. The fact that cell death related genes or pathways were not affected in the present study is in apparent contrast to the findings of Hanagata et al. (2011), who noted that genes related to cell cycle and cell death were deregulated in A549 lung carcinoma cells exposed to CuO NPs. Notwithstanding the fact that in vitro approaches using isolated cell types may not capture the orchestrated in vivo responses to NPs, it should also be noted that the A549 cell line is derived from a lung adenocarcinoma and may not be a faithful model of normal bronchial epithelium (Feliu et al., 2015) and that the study by Hanagata et al. (2011) was designed to assess acute toxicity, using relatively high doses and a short exposure time (24 hours), in contrast to our in vivo study in which rats were exposed for 5 consecutive days to a range of doses (low to high) (Gosens et al., 2016).

The present study does not specifically address whether the gene expression changes are due to the NPs themselves or to the ions released from the NPs. In our previously published study (Gosens et al., 2016) we addressed the issue of organ burden and particle deposition in the lungs and concluded that the CuO NPs were cleared

from the lungs during the 22 day post-exposure period through a combination of macrophage uptake and particle dissolution. We argued, based on dissolution experiments in artificial media and lung burden measurements that particle dissolution is not likely to occur immediately after deposition in the lung and that dissolution is more likely to occur in the acidic environment of the lysosomal compartment after macrophage uptake of the particles (Gosens et al., 2016). Nevertheless, the expression of genes related to metal homeostasis and detoxification, namely the metallothioneins, *Mt1a* and *Mt2a*, was only modestly upregulated according to the current microarray study, in comparison to genes involved in inflammation-related pathways. We also noted a minor decrease in the expression of *Mt1a* mRNA in liver tissue in the LD exposure group, but not at the higher dose, while no changes were observed in the lung tissue (see Supporting information). These results, together with the scant amount of copper deposits evidenced by our histochemical analysis, indicated that the Cu burden may be rapidly mitigated and that this may not be the direct causative trigger of the deleterious effects following inhalation. In fact, in our previous study, we could show that the Cu was cleared completely from the lungs within the recovery period (Gosens et al., 2016). In the aforementioned in vitro study by Hanagata et al. (2011), the authors argued that some of the gene expression changes in A549 cells were elicited by Cu ions released from the CuO NPs into the cell culture medium. Hence, of 648 genes upregulated by CuO NPs, 594 genes were suggested to be induced by CuO NPs themselves (or, potentially, by Cu ions released intracellularly), while 54 genes were

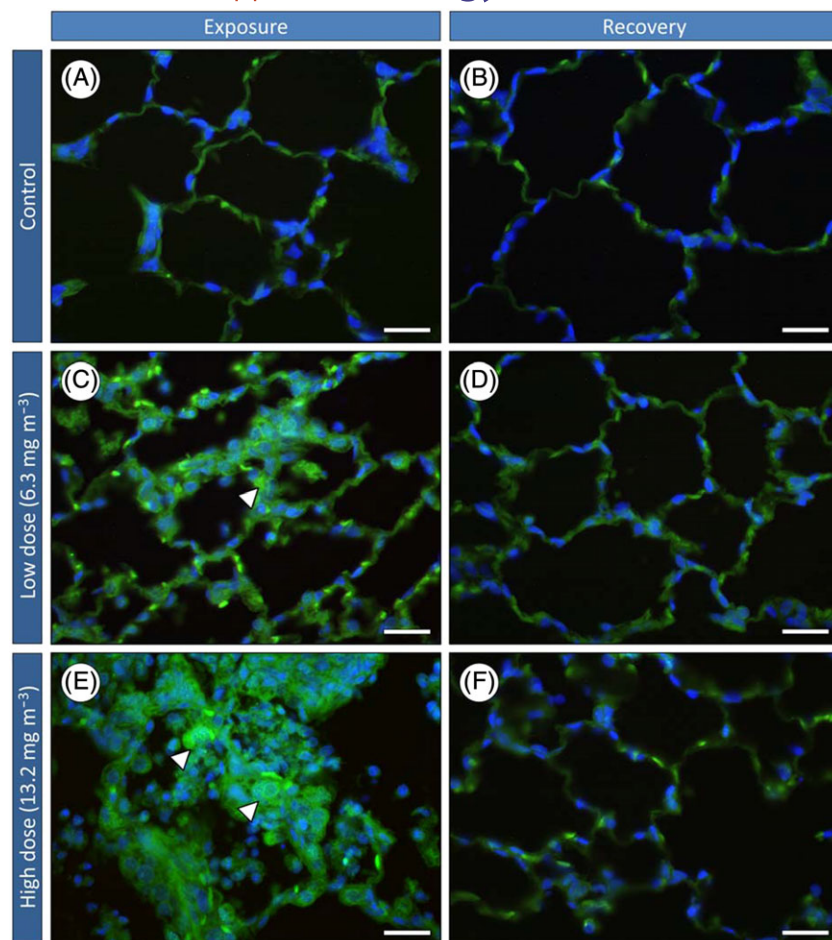


FIGURE 5 Expression of the cell proliferation marker, Ki67 in lung alveoli of control animals or rats exposed to CuO nanoparticles for 5 days and analyzed 1 day post-exposure and after a recovery period of 22 days (day 28). Lungs of rats exposed to clean air as a control (A,B) and after a low-dose exposure (C,D) or after a high-dose exposure (E,F). Arrows exemplify probe signals. Scale bars: 25 μm

attributable to Cu ions released from CuO NPs. Notably, several (nine) metallothionein genes were identified among the 54 genes that were upregulated both by CuO NPs and supernatants containing released Cu ions. Furthermore, in a very recent paper, Strauch, Niemand, Winkelbeiner, and Hartwig (2017) investigated the impact of micro- and nanosized CuO particles versus CuCl_2 using the human bronchial epithelial cell line, BEAS-2B, and A549 cells. They found that gene expression changes were most pronounced for CuO NPs as compared to microparticles and CuCl_2 , and gene expression analysis by RT-PCR revealed changes in metallothionein genes, oxidative stress genes and proinflammatory genes, as well as some cell death-related genes. However, it should be noted that there is a significant difference between such RT-PCR based studies in which a predefined panel of genes are investigated versus the present genome-wide transcriptomics approach, which allows for profiling of the entire genome. Nevertheless, the strong induction of metallothioneins in the study by Strauch et al. (2017) implied that the gene expression changes were caused by a release of Cu ions in the cells. In contrast to these in vitro studies, the present in vivo study showed low or modest induction of metallothionein-encoding genes in the lungs of exposed animals, arguing against a prominent role for released Cu ions in the current model.

We found that short-term exposure via inhalation to CuO NPs promoted overexpression of the ECT2 oncoprotein whose overexpression has previously been proposed as a prognostic biomarker for early-stage lung adenocarcinoma (Murata et al., 2014).

ECT2 expression was also associated with a poor prognosis for patients with non-small-cell lung cancers, and the induction of exogenous expression of ECT2 in fibroblasts or fibroblast-like cells promoted cellular invasive activity (Hirata et al., 2009). To this effect are added inflammation-related responses that we could also verify histologically. In fact, even though the alterations to lung bronchoalveolar tissue in rats exposed to CuO NPs were found to be reversible at 22 days post-exposure, the lesions were distributed as foci where infiltration of inflammatory cells and hyperplasia coincided, thus suggesting a link between the two effects: inflammation and proliferation of alveolar epithelial cells. The chemokine CCL2 (MCP-1) is a known chemotactic agent for monocytes and has been found to play a key role in mediating lung inflammation, for instance, following hypoxia (Chao, Donham, van Rooijen, Wood, & Gonzalez, 2011), cigarette smoking (Koth et al., 2010) and lipopolysaccharide challenge (Mercer et al., 2014). Moreover, CCL2 expression and recruitment of monocytes/macrophages are correlated with poor prognosis and metastatic disease in human breast cancer (Qian et al., 2011). The protein is secreted by a broad range of cells, which explains its localization within both immune and epithelial cells in the present study. Previous work has shown that welding-related metal oxide NPs trigger the production of proinflammatory cytokines and chemokines, including CCL2, in macrophage-like THP-1 cells (Andujar et al., 2014), while Brown, Johnston, Gubbins, and Stone (2014) reported that silica NPs, but not iron NPs, are potent inducers of CCL2 (MCP-1) secretion in the murine J774A.1 macrophage cell line. Moreover, Driscoll et al. (1996) reported that 90 day

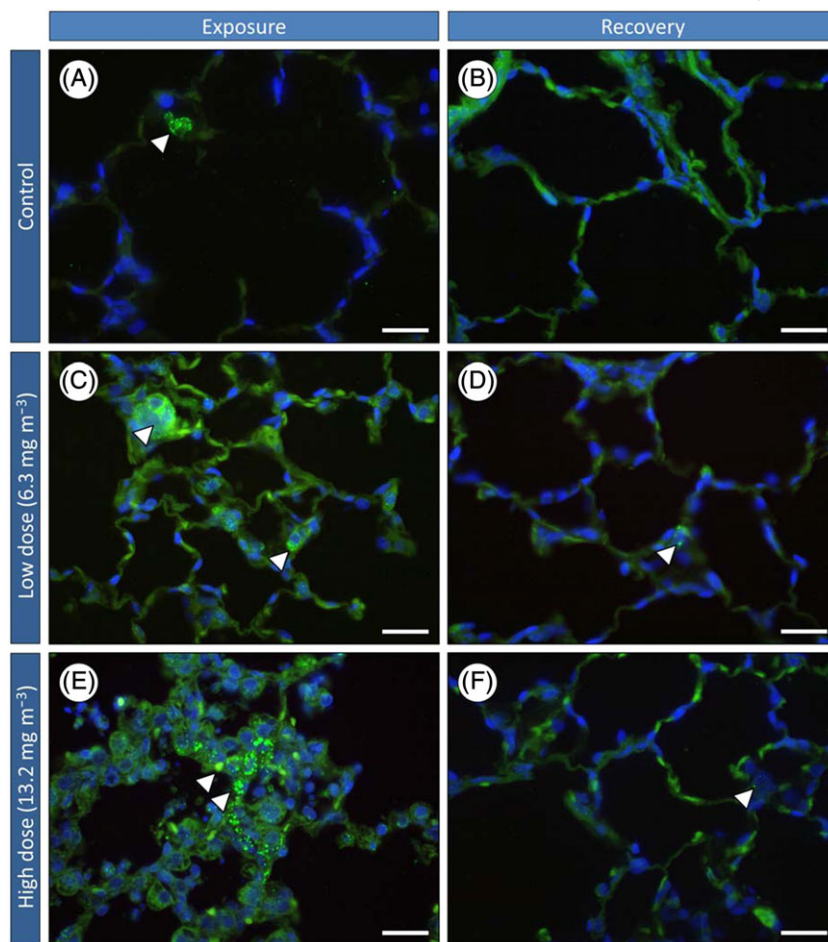


FIGURE 6 Expression of the chemokine, CCL2 in lung alveoli of control animals or rats exposed to CuO nanoparticles for 5 days and analyzed 1 day post-exposure and after a recovery period of 22 days (day 28). Lungs of rats exposed to clean air as a control (A,B) and after a low-dose exposure (C,D) or after a high-dose exposure (E,F). Arrows exemplify probe signals. Scale bars: 25 μm

inhalation exposure to carbon black resulted in a dose-dependent upregulation of MCP-1 mRNA with increased inflammation and alveolar epithelial cell hyperplasia. In the present work, a prominent (almost 90-fold) upregulation of the *Ccl2* gene was observed in HD-exposed animals. Additionally, the upregulation of CCL2 protein expression evidenced here supports a role of this molecule in the regulation of inflammatory processes following short-term inhalation to CuO NPs. Interestingly, in a recent bioinformatics study of transcriptomics data in public repositories, *Ccl2* was identified as a member of a group of genes related to pulmonary disease (fibrosis) following exposure to several different nanomaterials (Williams & Halappanavar, 2015). Altogether, these findings show that CCL2 may have a ubiquitous role in the activation of inflammatory responses (in the lungs) following NP challenge, specifically inhalation exposure of CuO NPs. In fact, the combination of lung alveolar hyperplasia and inflammation (phenotype level) and expression of *Ccl2* and *Ect2* (genotype level) may suggest a novel biomarker “footprint” and could guide the development of adverse outcome pathways (Sturla et al., 2014).

Epigenetic mechanisms of toxicity of nanomaterials, including changes to DNA methylation, histone modification and microRNA expression, have been postulated although the evidence is scant (Shyamasundar, Ng, Yung, Dheen, & Bay, 2015). Patil, Gade, and Deobagkar (2016) recently uncovered epigenetic alterations including DNA methylation changes in a lung fibroblast cell line in response to TiO_2 and ZnO NPs. Other recent studies demonstrated that alterations in gene-specific methylation corresponded with a pulmonary

inflammatory response to multiwalled carbon nanotubes in mice after 7 days of exposure, but not after acute (24 hours) exposure (Brown et al., 2016). Moreover, modest epigenetic effects, including global genome methylation changes, have also been described in the lungs of mice exposed to CuO NPs after only 24 hours, at doses that caused significant cellular damage in the lungs as evidenced by lactate dehydrogenase release (Lu et al., 2016). However, in the present study, the inflammatory response could not be explained by aberrant DNA methylation of inflammation-related genes, although a non-significant trend towards hypomethylation in the HD group at 1 day post-exposure (but not at recovery) was observed.

Taken together, the present study has confirmed that a short-term exposure via inhalation to CuO NPs causes acute inflammation in the lungs of rats and we could show, based on microarray analyses, that this coincides with proliferation of bronchoalveolar epithelium and upregulation of the oncoprotein ECT2 and the chemokine CCL2. Importantly, in spite of the known role of both ECT2 and CCL2 in lung neoplastic disease, as discussed above, no studies to date have been dedicated to their combined effects or interactions in tumorigenesis, or to their putative role in malignant transformation in bronchoalveolar epithelia following (long-term) exposure to NPs. The current study has shown that omics-based approaches provide a means to achieve a comprehensive and unbiased view of nanomaterial effects and may shed light on their mode of action, provided these tools are combined with adequate phenotypic anchoring of the data with assessment of

conventional endpoints of toxicity. As already highlighted, studies of the potential impact of long-term exposure to CuO NPs would be of interest.

ACKNOWLEDGEMENTS

The current work was supported by the European Commission through the Seventh Framework Programme project, FP7-SUN (grant agreement no. 604305), and through the Health Canada Genomics Research and Development Initiative. The authors wish to thank Ms. Dongmei Wu (Health Canada, Ottawa) for excellent technical support with the microarray analysis.

CONFLICT OF INTEREST

The authors did not report any conflict of interest.

ORCID

Bengt Fadeel  <http://orcid.org/0000-0001-5559-8482>

REFERENCES

- Andujar, P., Simon-Deckers, A., Galateau-Sallé, F., Fayard, B., Beaune, G., Clin, B., ... Lanone, S. (2014). Role of metal oxide nanoparticles in histopathological changes observed in the lung of welders. *Particle and Fibre Toxicology*, 11, 23.
- Benjamini, Y., & Hochberg, Y. (1995). Controlling the false discovery rate: A practical and powerful approach to multiple testing. *Journal of the Royal Statistical Society B*, 57, 289–300.
- Brown, D. M., Johnston, H., Gubbins, E., & Stone, V. (2014). Serum enhanced cytokine responses of macrophages to silica and iron oxide particles and nanomaterials: a comparison of serum to lung lining fluid and albumin dispersions. *Journal of Applied Toxicology*, 34, 1177–1187.
- Brown, D. M., Kanase, N., Gaiser, B., Johnston, H., & Stone, V. (2014). Inflammation and gene expression in the rat lung after instillation of silica nanoparticles: Effect of size, dispersion medium and particle surface charge. *Toxicology Letters*, 224, 147–156.
- Brown, T. A., Lee, J. W., Holian, A., Porter, V., Fredriksen, H., Kim, M., & Cho, Y. H. (2016). Alterations in DNA methylation corresponding with lung inflammation and as a biomarker for disease development after MWCNT exposure. *Nanotoxicology*, 10, 453–461.
- Chao, J., Donham, P., van Rooijen, N., Wood, J. G., & Gonzalez, N. C. (2011). Monocyte chemoattractant protein-1 released from alveolar macrophages mediates the systemic inflammation of acute alveolar hypoxia. *American Journal of Respiratory Cell and Molecular Biology*, 45, 53–61.
- Costa, P. M., & Fadeel, B. (2016). Emerging systems biology approaches in nanotoxicology: Towards a mechanism-based understanding of nanomaterial hazard and risk. *Toxicology and Applied Pharmacology*, 229, 101–111.
- Cui, X., Hwang, J. T. G., Qiu, J., Blades, N. J., & Churchill, G. A. (2005). Improved statistical tests for differential gene expression by shrinking variance components estimates. *Biostatistics*, 6, 59–75.
- Di Bucchianico, S., Fabrizio, M. R., Misra, S. K., Valsami-Jones, E., Berhanu, D., Reip, P., ... Migliore, L. (2013). Multiple cytotoxic and genotoxic effects induced in vitro by differently shaped copper oxide nanomaterials. *Mutagenesis*, 28, 287–299.
- Driscoll, K. E., Carter, J. M., Howard, B. W., Hassenbein, D. G., Pepelko, W., Baggs, R. B., & Öbersdörster, G. (1996). Pulmonary inflammation, chemokine, and mutagenic responses in rats after subchronic inhalation of carbon black. *Toxicology and Applied Pharmacology*, 136, 372–380.
- Fahmy, B., & Cormier, S. A. (2009). Copper oxide nanoparticles induce oxidative stress and cytotoxicity in airway epithelial cells. *Toxicology In Vitro*, 23, 1365–1371.
- Feliu, N., Kohonen, P., Ji, J., Zhang, Y., Karlsson, H. L., Palmberg, L., ... Fadeel, B. (2015). Next-generation sequencing reveals low-dose effects of cationic dendrimers in primary human bronchial epithelial cells. *ACS Nano*, 9, 146–163.
- Gioria, S., Lobo Vicente, J., Barboro, P., La Spina, R., Tomasi, G., Urbán, P., ... Chassaigne, H. (2016). A combined proteomics and metabolomics approach to assess the effects of gold nanoparticles in vitro. *Nanotoxicology*, 10, 736–748.
- Gosens, I., Cassee, F., Zenalla, M., Manodori, L., Brunelli, A., Costa, A. L., ... Stone, V. (2016). Organ burden and pulmonary toxicity of nanosized copper (II) oxide particles after short-term inhalation exposure. *Nanotoxicology*, 10, 1084–1095.
- Halappanavar, S., Saber, A. T., Decan, N., Jensen, K. A., Wu, D., Jacobsen, N. R., ... Vogel, U. (2015). Transcriptional profiling identifies physico-chemical properties of nanomaterials that are determinants of the in vivo pulmonary response. *Environmental and Molecular Mutagenesis*, 56, 245–264.
- Hanagata, N., Zhuang, F., Connolly, S., Li, J., Ogawa, N., & Xu, M. (2011). Molecular responses of human lung epithelial cells to the toxicity of copper oxide nanoparticles inferred from whole genome expression analysis. *ACS Nano*, 5, 9326–9338.
- Hartung, T., FitzGerald, R. E., Jennings, P., Mirams, G. R., Peitsch, M. C., Rostami-Hodjegan, A., ... Sturla, S. J. (2017). Systems toxicology: Real world applications and opportunities. *Chemical Research in Toxicology*, 30, 870–882.
- Hirata, D., Yamabuki, T., Miki, D., Ito, T., Tsuchiya, E., Fujita, M., ... Daigo, Y. (2009). Involvement of epithelial cell transforming sequence-2 oncoantigen in lung and esophageal cancer progression. *Clinical Cancer Research*, 15, 256–266.
- Hosack, D. A., Dennis, G. Jr., Sherman, B. T., Lane, H. C., & Lempicki, R. A. (2003). Identifying biological themes within lists of genes with EASE. *Genome Biology*, 4, R70.
- Huang, D. W., Sherman, B. T., & Lempicki, R. A. (2009a). Systematic and integrative analysis of large gene lists using DAVID bioinformatics resources. *Nature Protocols*, 4, 44–57.
- Huang, D. W., Sherman, B. T., & Lempicki, R. A. (2009b). Bioinformatics enrichment tools: Paths toward the comprehensive functional analysis of large gene lists. *Nucleic Acids Research*, 37, 1–13.
- Ihaka, R., & Gentleman, R. (1996). R: A language for data analysis and graphics. *Journal of Computational and Graphical Statistics*, 5, 299–314.
- Jing, X., Park, J. H., Peters, T. M., & Thorne, P. S. (2015). Toxicity of copper oxide nanoparticles in lung epithelial cells exposed at the air-liquid interface compared with in vivo assessment. *Toxicology In Vitro*, 29, 502–511.
- Kanehisa, M., Goto, S., Sato, Y., Kawashima, M., Furumichi, M., & Tanabe, M. (2014). Data, information, knowledge and principle: Back to metabolism in KEGG. *Nucleic Acids Research*, 42, D199–D205.
- Karlsson, H. L., Cronholm, P., Gustafsson, J., & Möller, L. (2008). Copper oxide nanoparticles are highly toxic: A comparison between metal oxide nanoparticles and carbon nanotubes. *Chemical Research in Toxicology*, 21, 1726–1732.
- Karlsson, H. L., Toprak, M. S., & Fadeel, B. (2015). Toxicity of metal and metal oxide nanoparticles. In G. F. Nordberg, B. A. Fowler, & M. Nordberg (Eds.), *Handbook on the Toxicology of Metals* (4th ed.). Amsterdam: Academic Press-Elsevier, 75–112.
- Kerr, M. K., & Churchill, G. A. (2007). Statistical design and the analysis of gene expression microarray data. *Genetical Research*, 89, 509–514.
- Koth, L. L., Cambier, C. J., Ellwanger, A., Solon, M., Hou, L., Lanier, L. L., ... Woodruff, P. G. (2010). DAP12 is required for macrophage recruitment to the lung in response to cigarette smoke and chemotaxis toward CCL2. *Journal of Immunology*, 184, 6522–6245.
- Krämer, C., Green, J., Pollard, J., & Tugeneich, S. (2014). Causal analysis approaches in ingenuity pathway analysis. *Bioinformatics*, 30, 523–530.

- Kuhlbusch, T. A., Asbach, C., Fissan, H., Gohler, D., & Stintz, M. (2011). Nanoparticle exposure at nanotechnology workplaces: A review. *Particle and Fibre Toxicology*, 8, 22.
- Lin, C., Song, H., Huang, C., Yao, E., Gacayan, R., Xu, S.-M., & Chuang, P. T. (2012). Alveolar type II cells possess the capability of initiating lung tumor development. *PLoS One*, 7, e53817.
- Lu, X., Miousse, I. R., Pirela, S. V., Moore, J. K., Melnyk, S., Koturbash, I., & Demokritou, P. (2016). In vivo epigenetic effects induced by engineered nanomaterials: a case study of copper oxide and laser printer-emitted engineered nanoparticles. *Nanotoxicology*, 10, 629–639.
- Lucafò, M., Gerdol, M., Pallavicini, A., Pacor, S., Zorzet, S., Da Ros, T., ... Sava, G. (2013). Profiling the molecular mechanism of fullerene cytotoxicity on tumor cells by RNA-seq. *Toxicology*, 314, 183–192.
- Martins, C., Alves de Matos, A. P., Costa, M. H., & Costa, P. M. (2015). Alterations in juvenile flatfish gill epithelia induced by sediment-bound toxicants: A comparative in situ and ex situ study. *Marine Environmental Research*, 112, 122–130.
- Mercer, P. F., Williams, A. E., Scotton, C. J., José, R. J., Sulikowski, M., Moffatt, J. D., ... Chambers, R. C. (2014). Proteinase-activated receptor-1, CCL2, and CCL7 regulate acute neutrophilic lung inflammation. *American Journal of Respiratory Cell Molecular Biology*, 50, 1441–1457.
- Moffat, I., Chepelev, N. L., Labib, S., Bourdon-Lacombe, J., Kuo, B., Buick, J. K., ... Yauk, C. L. (2015). Comparison of toxicogenomics and traditional approaches to inform mode of action and points of departure in human health risk assessment of benzo[a]pyrene in drinking water. *Critical Reviews in Toxicology*, 45, 1–43.
- Murata, Y., Minami, Y., Iwaka, R., Yokota, J., Usui, S., Tsuta, K., ... Noguchi, M. (2014). ECT2 amplification and overexpression as a new prognostic biomarker for early-stage lung adenocarcinoma. *Cancer Science*, 105, 490–497.
- Nikola, J., Williams, A., Yauk, C. L., Wallin, H., Vogel, U., & Halappanavar, S. (2016). Meta-analysis of transcriptomic responses as a means to identify pulmonary disease outcomes for engineered nanomaterials. *Particle and Fibre Toxicology*, 13, 25.
- Ohshima, Y., Kurabayashi, M., Masuda, H., Nakamura, T., Aihara, Y., Kaname, T., ... Nagai, R. (1998). Molecular cloning of rat klotho cDNA: Markedly decreased expression of klotho by acute inflammatory stress. *Biochemical and Biophysical Research Communications*, 251, 920–925.
- Patil, N. A., Gade, W. N., & Deobagkar, D. D. (2016). Epigenetic modulation upon exposure of lung fibroblasts to TiO₂ and ZnO nanoparticles: Alterations in DNA methylation. *International Journal of Nanomedicine*, 11, 4509–4519.
- Perreault, F., Melegari, S. P., da Costa, C. H., Franco Rossetto, A. L. O., Popovic, R., & Matias, W. G. (2012). Genotoxic effects of copper oxide nanoparticles in neuro 2A cell cultures. *Science of the Total Environment*, 441, 117–124.
- Qian, B.-Z., Li, J., Zhang, H., Kitamura, T., Zhang, J., Campion, L. R., ... Pollard, J. W. (2011). CCL2 recruits inflammatory monocytes to facilitate breast-tumour metastasis. *Nature*, 475, 222–227.
- Rinaldo, M., Andujar, P., Lacourt, A., Martinon, L., Canal Raffin, M., Dumortier, P., ... Brochard, P. (2015). Perspectives in biological monitoring of inhaled nanosized particles. *Annals of Occupational Hygiene*, 59, 669–680.
- Schlüter, C., Duchrow, M., Wohlenberg, C., Becker, M. H. G., Key, G., Flad, H. D., & Gerdes, J. (1993). The cell proliferation-associated antigen of antibody Ki-67: A very large, ubiquitous nuclear protein with numerous repeated elements, representing a new kind of cell cycle-maintaining proteins. *Journal of Cell Biology*, 123, 513–522.
- Schroeder, A., Mueller, O., Stocker, S., Salowsky, R., Leiber, M., Gassmann, M., ... Ragg, T. (2006). The RIN: An RNA integrity number for assigning integrity values to RNA measurements. *BMC Molecular Biology*, 7, 3.
- Seaton, A., MacNee, W., Donaldson, K., & Godden, D. (1995). Particulate air pollution and acute health effects. *Lancet*, 345, 176–178.
- Servant, N., Gravier, E., Gestraud, P., Laurent, C., Paccard, C., Biton, A., ... Hupé, P. (2010). EMA – A R package for easy microarray data analysis. *BMC Research Notes*, 3, 277.
- Shyamasundar, S., Ng, C. T., Yung, L. Y., Dheen, S. T., & Bay, B. H. (2015). Epigenetic mechanisms in nanomaterial-induced toxicity. *Epigenomics*, 7, 395–411.
- Strauch, B. M., Niemand, R. K., Winkelbeiner, N. L., & Hartwig, A. (2017). Comparison between micro- and nanosized copper oxide and water soluble copper chloride: Interrelationship between intracellular copper concentrations, oxidative stress and DNA damage response in human lung cells. *Particle and Fibre Toxicology*, 14, 28.
- Sturla, S. J., Boobis, A. R., Fitzgerald, R. E., Hoeng, J., Kavlock, R. J., Schirmer, K., ... Peitsch, M. C. (2014). Systems toxicology: From basic research to risk assessment. *Chemical Research in Toxicology*, 27, 314–329.
- Tatsumoto, T., Xie, X., Blumenthal, R., Okamoto, I., & Miki, T. (1999). Human ECT2 is an exchange factor for rho GTPases, phosphorylated in G2/M phases, and involved in cytokinesis. *Journal of Cell Biology*, 147, 921–928.
- Tuomela, S., Autio, R., Buerki-Thurnherr, T., Arslan, O., Kunzmann, A., Andersson-Willman, B., ... Lahesmaa, R. (2013). Gene expression profiling of immune-competent human cells exposed to engineered zinc oxide or titanium dioxide nanoparticles. *PLoS One*, 8, e68415.
- Williams, A., & Halappanavar, S. (2015). Application of biclustering of gene expression data and gene set enrichment analysis methods to identify potentially disease causing nanomaterials. *Beilstein Journal of Nanotechnology*, 6, 2438–2448.
- Labib, S., Williams, A., Yauk, C. L., Nikola, J. K., Wallin, H., Vogel, U., & Halappanavar, S. (2016). Nano-risk science: Application of toxicogenomics in an adverse outcome pathway framework for risk assessment of multi-walled carbon nanotubes. *Particle and Fibre Toxicology*, 13, 15.
- Wilson, V. S., Keshava, N., Hester, S., Segal, D., Chiu, W., Thompson, C. M., & Euling, S. Y. (2013). Utilizing toxicogenomic data to understand chemical mechanism of action in risk assessment. *Toxicology and Applied Pharmacology*, 271, 299–308.
- Wu, H., Kerr, K., Cui, X., & Churchill, G. A. (2003). MAANOVA: a software package for the analysis of spotted cDNA microarray experiments. In G. Parmigiani, E. S. Garrett, R. A. Irizarry, & S. L. Zeger (Eds.), *The Analysis of Gene Expression Data: Methods and Software*. New York: Springer, 313–341.

SUPPORTING INFORMATION

Additional Supporting Information may be found online in the supporting information tab for this article.

How to cite this article: Costa PM, Gosens I, Williams A, et al. Transcriptional profiling reveals gene expression changes associated with inflammation and cell proliferation following short-term inhalation exposure to copper oxide nanoparticles. *J Appl Toxicol*. 2018;38:385–397. <https://doi.org/10.1002/jat.3548>